ELSEVIER

International Journal of Mass Spectrometry 200 (2000) 219–241

International Journal of Mass Spectrometry

Kinetic energy dependence of ion–molecule reactions: guided ion beams and threshold measurements

P.B. Armentrout

Department of Chemistry, University of Utah, Salt Lake City, UT 84112, USA

Received 6 June 2000; accepted 14 August 2000

Abstract

Over the past 20 years, ion beam methods have become a reliable experimental tool for the determination of thermochemical data. Confidence in these methods has required the synergistic development of improved instrumentation and enhanced analysis techniques. Guided ion beams, as introduced by Teloy and Gerlich in 1974 [Chem. Phys. 4 (1974) 417], have revolutionized our ability to measure accurate integral cross sections of ion–molecule reactions throughout the energy range of chemical interest. Such high quality data have then necessitated empirical and theoretical advances in our understanding of the kinetic energy dependence of chemical reactions. This need has led to increasingly sophisticated models that permit the extraction of meaningful thermodynamic values from the analysis of kinetic energy dependent data. Key contributions in the development of both advances are reviewed here. (Int J Mass Spectrom 200 (2000) 219–241) © 2000 Elsevier Science B.V.

Keywords: Bond energies; Guided ion beams; Octopole; Thermochemistry; Thresholds

1. Introduction

Twenty years ago, the use of ion beam methods to measure thermodynamic information was in its infancy. Thermodynamic compilations from this era do not even mention information from reaction threshold measurements, in contrast to threshold measurements of ionization energies and appearance energies, which were abundant [1]. Now, it is generally conceded that ion beam methods are a reliable tool for extracting thermodynamic information on a broad variety of chemical species. It is the purpose of this article to try to document, largely from my own personal perspective, how ion beam measurements came to realize this level of respectability.

There are two synergistic parts to this story: the development of guided ion beam methods by Teloy and Gerlich, introduced in 1974 [2,3], and the gradual improvement of our understanding of how kinetic and internal energy drives endothermic reactions. Ion guides provided the hardware needed to accurately study the kinetic energy dependence of ion–molecule reactions over a broad range of energies that encompass the chemically interesting region (thermal to tens of electron volts). The improved understanding led to the analytic tools necessary to interpret the observed kinetic energy dependent cross sections in useful ways. Specifically, means to measure the kinetic energy thresholds of endothermic reactions have been devised, and the relationship of these thresholds to

* E-mail: armentrout@chemistry.chem.utah.edu

PII S1387-3806(00)00310-9

thermodynamic data has been established. In many cases, the thermodynamic values obtained are in good agreement with values obtained by more traditional thermodynamic methods. In many others, no comparable information is available in the literature.

Although threshold measurements of ion–molecule reactions can be performed with many types of instrumentation, the link between such studies and guided ion beam techniques is a strong one. Indeed, the NIST Webbook [4] states in its section on "Determinations of Reaction Endothermicity" that "more commonly a so-called guided beam apparatus is utilized for such determinations."

2. Guided ion beam methods

Experiments involving the reactions of ion beams can generally be classified in one of four categories: beam–gas, crossed beams, merged beams, and guided beam. These methods have been nicely reviewed in several articles over the years [5–7]. The latter experiment is the youngster of the bunch and was introduced by Teloy and Gerlich in 1974 [3]. However, results from this intriguing new method were slow to reach the literature with only two additional publications in the primary literature in the following decade [8,9]. Nevertheless, these early results convincingly demonstrated that the guided ion beam technique opened new horizons on the ability to measure integral cross sections over a wide range of kinetic energies with excellent sensitivity. (I remember my excitement as a graduate student when I first saw the exquisite data in the article of Frobin et al. [9]. I told myself then that this certainly was the way to measure the kinetic energy dependence of cross sections and obtain meaningful results.) Although details of the dynamics intrinsic to the angularly resolved differential cross sections obtained by crossed beam methods are lost, integral cross sections allow the kinetic energy dependence of reactions to be monitored with sensitivity and fidelity. Traditional merged beam techniques also allow kinetic energy studies over broad energy ranges including down to very low relative energies [10,11]. However, the experimental difficulties associated with traditional merged beam techniques are amply discussed elsewhere [5–7] and limit the applicability of such methods to a wide range of species, sufficiently so that relatively few merged beam studies are presently conducted. (However, an apparatus built by Gerlich [12] in which merged beam and guided beam techniques are combined overcomes many of these difficulties.)

Before the advent of guided beam methods, reaction threshold measurements were generally conducted using beam–gas methods. Both types of instruments exist in many experimental variations and the key difference between them is whether the collision region, in which the ion–molecule reactions of interest take place, incorporates a rf-only ion beam guide. These devices solve the two most vexing problems associated with integral cross-section measurements in beam–gas experiments: (1) efficient collection of all products, and (2) access to low energies (below about 1 eV in the laboratory).

The theory of ion guides and the myriad of ways in which they can be built and used are described in an excellent, practical review by Gerlich [12]. In keeping with common usage, I define guided beam experiments as those in which the reactions of interest occur inside a rf-only beam guide of six or more poles (where the octopole is the most common configuration) that cylindrically surround the ion beam path. This definition excludes the use of rf beam guides for simply transporting ions from a source to a reaction region such as a drift tube [13] or an ion cyclotron resonance (ICR) mass spectrometer [14,15] and the triple quadrupole mass spectrometers in which the central quadrupole is a rf-only device [16]. Further, this retrospective will not include an examination of spectroscopic or photodissociation experiments conducted in ion guides: see, e.g. [17–20].

Classical mechanics [21] shows that when charged particles are in an inhomogeneous potential field that oscillates more rapidly than the time it takes the particles to move between electrodes, the particles are trapped in a pseudopotential well that is flat near the center of the electrode array and rises steeply near the electrodes. For a device containing $2n$ electrodes (or poles), this effective potential is given by

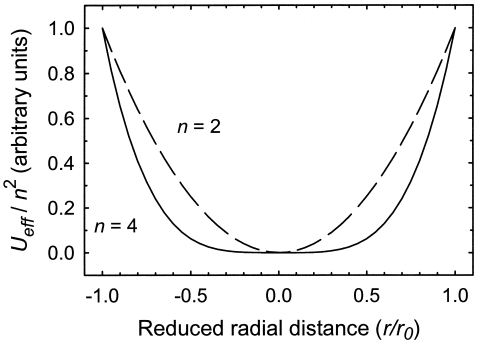

Fig. 1. Relative effective potential as a function of the reduced radial distance given by Eq. (1) and scaled by n^2 for a quadrupole ($n = 2$) and an octopole ($n = 4$) system.

$$U_{eff}(r) = [n^2q^2V_0^2/(4m\omega^2r_0^2)](r/r_0)^{2n-2} \quad (1)$$

where r is the radial distance from the centerline, r_0 is the inscribed radius of the multipole, the particle has mass m and charge q, and the rf amplitude is V_0 with a frequency of ω. For an octopole ($n = 4$), the effective radial potential varies as r^6, Fig. 1, such that the guide has a large tubular trapping volume with steep walls near the poles. In contrast, a quadrupole ($n = 2$) has a quadratic potential (r^2) which yields large perturbations on the kinetic energy and less effective trapping. (For the same applied rf field, a quadrupole has a maximum trapping potential that is one-fourth that of an octopole field.) Therefore, whereas rf-only quadrupoles present some of the same virtues as higher order multipoles, their use in kinetic energy resolved measurements leads to collision energies that are not as well defined.

In any such devices, however, the energy of the ion along the axis of the guide is unaffected, i.e. the ion guide acts as a radial trap of the ions. Hence, the radial field traps products formed in collisions occurring inside the ion guide such that they can be efficiently collected, regardless of their scattering angle. This collection efficiency accounts for the increased sensitivity of guided beam experiments. In addition, the primary reason that ion experiments historically could not access regions below about 1 eV in the laboratory frame is that slow moving ions would disperse because of space charge effects (coulombic repulsion). As long as such dispersion occurs inside the ion guide, the ions still move forward with well-defined energies but are trapped such that there is no loss in intensity. This radial trapping permits the use of routine retarding potential measurements of the kinetic energy, historically a very difficult task [22]. Further, kinetic energies close to thermal (0.03 eV at 300 K) and up to kilovolts can easily be accessed using ion beam guides. An early example from our laboratory is shown in Fig. 2 [23]. Here, the cross sections have been converted to rate constants using the relationship,

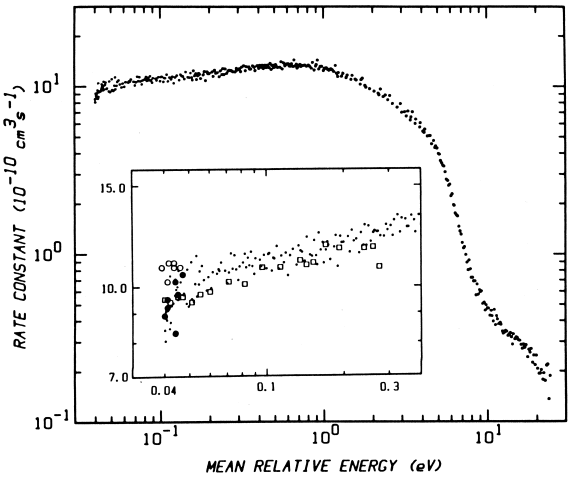

Fig. 2. Phenomenological rate constants, Eq. (2), for the reaction $Ar^+ + H_2 \rightarrow ArH^+ + H$ as a function of the mean relative energy of the reactants, $\langle E \rangle$. The small points show the guided ion beam results of [23]. The inset compares this data to flow/drift results in an argon buffer (closed circle [26]; open circle [27]) and a helium buffer (open square [27]). Reprinted from [23] with permission.

$$k(\langle E \rangle) = \sigma(E)\,\nu \quad (2)$$

where v is the relative velocity of the reactants and $\langle E \rangle = E + (3/2)\gamma k_B T$,where k_B is Boltzmann's constant, T is the temperature of the reactant neutral, $\gamma = M_I/(M_N + M_I)$, and M_N and M_I are the masses of the neutral and ionic reactants, respectively. The latter term in the expression for $\langle E \rangle$ accounts for the average kinetic energy of the neutral reactant. Fig. 3 shows results for this same system extended another factor of 30 lower in energy using combined merged-guided beam methods [24]. Results for a combined crossed beam–guided beam experiment are also shown [25].

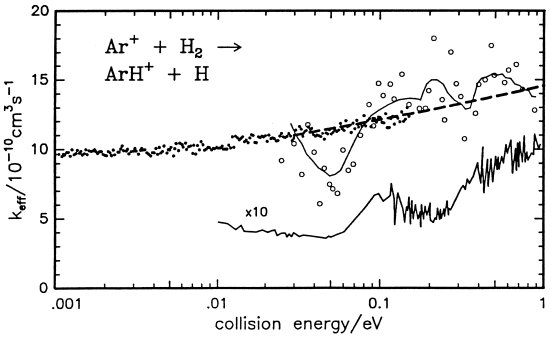

Fig. 3. Effective rate constants for the reaction $Ar^+ + H_2 \rightarrow ArH^+ + H$ as a function of the relative collision energy of the reactants. The dashed line shows the guided ion beam gas cell experiments of Fig. 2. The small points are the merged beam-guided beam results of Gerlich [24]. The open circles indicate the crossed beam-guided beam results of Tosi et al. [25], which have been fitted with a structured trial function (upper line). The lower line is a calculated cross section augmented by a factor of 10 for better comparison. Reprinted from [24] with permission.

Thus, guided beam methods allow the entire gamut of chemically interesting energies, ranging from very low to much higher than is needed to make and break chemical bonds, is available to ion beam instruments with no loss of sensitivity inherent in beam–gas arrangements.

Fig. 2 shows very good agreement between the guided ion beam results and flow/drift tube measurements [26,27]. Further, good agreement among the results of three independent guided ion beam studies is found in Fig. 3 (although the difference in the merged versus crossed beam studies, which should both have higher energy resolution than our guided ion beam–gas cell measurements, is not completely understood [24]). This agreement shows the high reliability of the absolute cross sections and resultant rate constants. Indeed, our initial intent in measuring the $Ar^+ + H_2$ reaction cross section was simply to calibrate the length of our reaction cell, l, one of the key unknowns in determining absolute cross sections. Conversion of raw ion intensity data to cross sections is accomplished using the equation $\sigma(E) = -(RT/Pl)\ln(I/I_0)$, where I and I_0 are the reactant ion intensities after and before reaction, respectively, R is the gas constant, and P is the pressure of the neutral gas. We first estimated the length of the collision cell using standard approximations [28,29] and found that the resultant absolute cross sections agreed extremely well with all literature information, both thermal and near-thermal rate constants [26,27], Fig. 2, and previous beam measurements at higher energies [3,5,30–34], Fig. 4. Indeed, this measurement has proven to be sufficiently robust that it is often used by others seeking to calibrate the length of their interaction region. A more stringent test of the accuracy of these absolute cross sections is a comparison to theory. A good example is the reaction of $O^+(^4S) + H_2 \rightarrow OH^+ + H$ (and its isotopic variants with HD and D_2), which is exothermic, barrierless, and occurs on a single potential energy surface such that it is expected to follow the Langevin-Gioumousis-Stevenson collision cross section [35,36]. Our results for the H_2, HD, and D_2 systems fell within 10% of the predicted cross sections over an extended energy range down to about 0.01 eV [37]. These differences are well within the 20% absolute uncertainty estimated for our cross sections.

Blessed with our present hindsight, it is interesting to revisit the early reviews of the relative merits of the guided ion beam technique. Henchman, whose review was published in 1972 [5], had only the earliest works of Teloy and Gerlich available to him [2]. He recognized the strengths of guided ion beams as the ability to measure reaction cross sections (as compared to rate constants), the large energy range available, the good energy definition, and the high product detection efficiency. He identified disadvantages of the method as relatively poor ability to identify ionic reactants and their states. In Gentry's review of 1979 [6], the same set of strengths was identified (sensitivity, accuracy, and energy range), although he finds the ability to control internal states to be an advantage. Gentry notes that the resolution of reactant kinetic energy, product kinetic energy, and scattering angle are poor, and assesses the range of systems amenable to study to be only moderate (5 on a 10 point scale). Thus, both Henchman and Gentry point to reactant identity and reaction system versatility as limitations of the early guided beam methods. By 1988, Farrar [7] notes that these limitations have disappeared and points to "the addition of mass selection of the primary ion beam by Ervin and Armentrout" [23] as

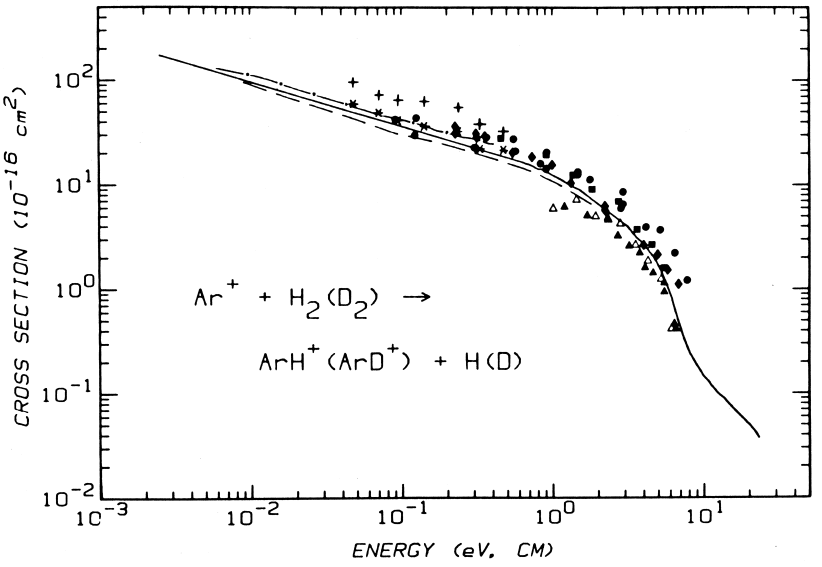

Fig. 4. Cross sections for the reaction $Ar^+ + H_2$ (D_2) → ArH^+ (ArD^+) + H (D) as a function of the center-of-mass ion energy, *E*. The lines show guided ion beam results from [23] (solid line) and from [3] (upper dashed line, H_2; lower dashed line, D_2). Beam–gas results are given by open symbols for H_2 and solid symbols for D_2: closed circle, Henchman [5]; closed diamond, Hyatt et al. [33]; closed square, Homer et al. [32]; closed and open triangle, Henglein and co-workers [30,31]; state-specific results for $Ar^+(^2P_{3/2})$ and $Ar^+(^2P_{1/2})$ + H_2 are given by an asterisk and a plus sign, respectively, Tanaka et al. [34]. Reprinted from [23] with permission.

"a key extension of the guided beam method, opening up the possibility of studying a much wider range of chemical phenomena than had been possible heretofore." (Truthfully, one of the early versions of the apparatus of Teloy and Gerlich [3] also incorporated a rf mass filter for the primary ions of rather unique design, but this device did not have particularly high mass resolution.) Similar advances occurred rapidly in other laboratories such that at present, it is probably fair to say that guided ion beam methods have been applied to more ion–molecule systems than merged beams, crossed beams, or beam–gas methods, although this personal assessment is difficult to quantify with any accuracy.

Certainly, the versatility of guided ion beam measurements is without question, and has been enhanced by the ability to couple a host of external ion sources to guided beam reaction regions. These include ion sources utilizing electron impact ionization, surface ionization, photoionization, multiphoton ionization, laser ablation, sputtering, glow discharge, and microwave discharge as means of ionization; all of which can then be combined with ion thermalization in rf storage devices, flow tubes, and supersonic expansions. Both positive and negative ions [38–41] from atom–diatom to complex chemical processes have been studied. Impressive state-specific reaction dynamics have been explored in guided ion beam systems for specific electronic states of atomic ions prepared by photoionization [42] and specific vibrational states for small molecular ions formed by photoionization [42,43] and multiphoton methods [44,45]. My group has utilized the comparison of ions produced in several types of sources (surface ionization, electron ionization, and flow tube sources) to examine the variations in reactivity of specific electronic state of atomic transition metal ions [46]. Metal clusters [47–50], organometallic species [51], and various solvated ions [52] have all been studied using guided beam methods. To dramatically lower the relative kinetic energy distributions (see Sec. 3.1 on Doppler broadening), crossed neutral beams have been incorporated in guided ion beam instruments [53–55]. The recent advent of a high temperature reaction cell has further enhanced the range of systems amenable to study to those where the neutral

reactant is a metal atom [56,57]. Sublemontier et al. [58] have recently coupled time-of-flight mass spectrometers to an octopole reaction zone. These and other guided ion beam instruments used for reaction studies [59–61] demonstrate the tremendous range of systems accessible to the method.

It should also be mentioned that the "inability" of guided beam methods to determine product velocities and angular distributions may have been true in its original incarnation, but such an assessment is presently without merit. Product velocities along the axis of the ion guide can be measured very accurately using time-of-flight methods. As discussed thoroughly by Gerlich [12], it is also straightforward to determine the radial velocities by variation of the rf amplitude applied to the guide. This variation systematically varies the depth of the trapping well allowing ions with radial velocities above the potential well depth to escape. Combination of these axial and radial velocity measurements provides all the information needed for a determination of differential cross sections. Although the angular resolution of such measurements does not approach that accessible in true crossed beam studies [62], several groups have now determined low-resolution differential scattering cross sections for bimolecular reactions [12,63–67] and photodissociation processes [68]. An example is shown in Fig. 5 for the reaction of OCS^+ in its ground vibrational and electronic state reacting with C_2H_2 to form $C_2H_2S^+ + CO$ [67]. Clear forward/backward scattering is observed at both the lowest and highest collision energies examined. Such information provides sufficient detail to allow the dynamics of the reactions studied to be assessed.

3. Measurement of reaction thresholds

The earliest study of endothermic ion–molecule reactions was that of Giese and Maier [69] who used a tandem mass spectrometer to study the endothermic dissociative ionization processes, where Rg = Ne and Ar

$$Rg^+ + CO \rightarrow C^+ + O + Rg \quad (3)$$

These authors immediately recognized "that the technique used may prove useful for determining unknown bond-dissociation energies," but also realized the limitations imposed by the lack of theory for the energy dependence of reaction cross sections. Several additional articles on endothermic dissociative ionization processes followed [70,71]. In these studies, threshold behavior was interpreted in terms of a semiempirical formula for the reaction cross section with $m = 1/2$,

$$\sigma(E) = \sigma_0(E - E_0)^n/E^m \quad (4)$$

where E is the kinetic energy of the reactants in the center-of-mass frame, σ_0 is an energy independent scaling factor, and E_0 is the threshold for reaction. Maier [72] then reported the first study of an endothermic ion–molecule reaction involving atom transfer,

$$C^+ + D_2 \rightarrow CD^+ + D \quad (5)$$

The energy scale for these data was shifted such that a linear extrapolation of the data yielded an intercept consistent with the known endothermicity of reaction (5) at the time, namely, 0.4 eV. These results were interpreted by using phase space theory results of Light [73] and Pechukas and Light [74], which predicted that ion–molecule reaction cross sections should vary as $(E - E_0)$ and $(E - E_0)^{5/4}$, respectively.

3.1. Doppler broadening

Unfortunately, the quantitative interpretation of these early results was hindered because these authors did not realize the substantial effect of the neutral reactant motion on their experiments. A critical contribution to this field was the theoretical treatment of this motion and its influence on reaction cross sections, so-called "Doppler broadening," by Chantry [75]. He reinterpreted the results of Maier for reaction (5) using a phase-space theoretical prediction of Truhlar [76], which he reproduced by using the semiempirical formula,

$$\sigma(E) = \sigma_0\{1 - \exp[-A(E - E_0)]\} \quad (6)$$

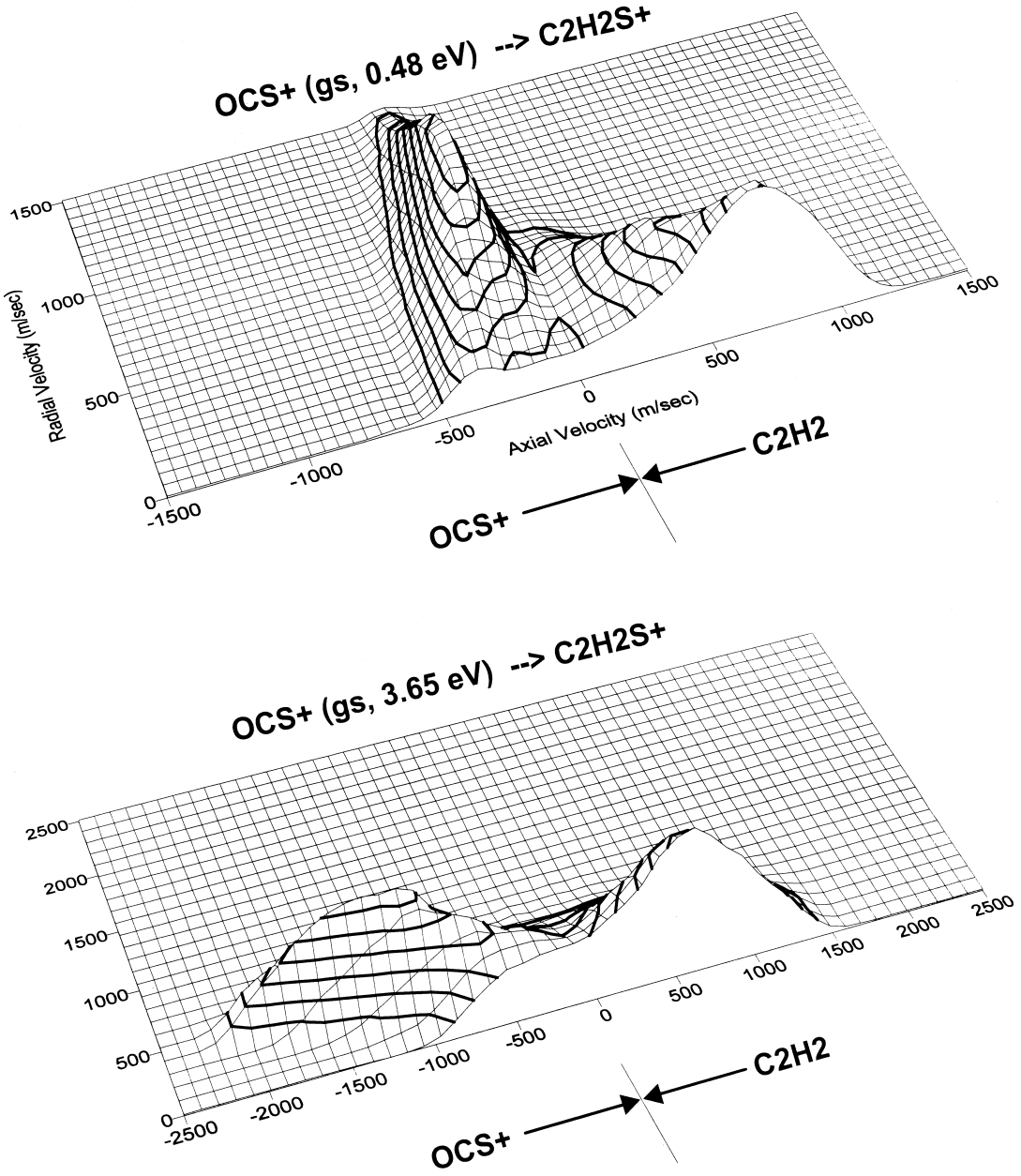

Fig. 5. Simulated velocity distributions for $C_2H_2S^+$ product ions from reaction of $OCS^+ + C_2H_2$ at two collision energies, as shown. Reprinted from [67] with permission.

where *A* is an adjustable parameter and all other quantities are the same as for Eq. (4). Accurate modeling of the data necessitated shifting the cross sections such that they were closer to the original energy scale. Thus, it was shown that the cross section rose much more rapidly than the data and that the real threshold was actually substantially higher than the apparent threshold of the data. The importance of this effect and its subtleties are illustrated by early guided ion beam results from my laboratory [77], shown in

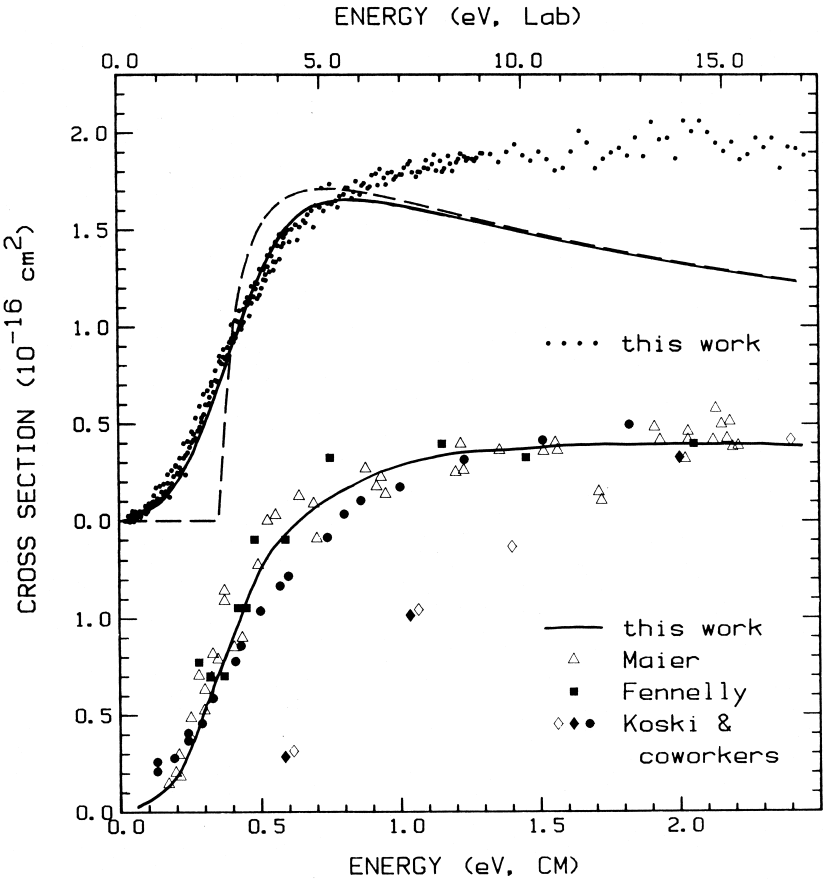

Fig. 6. Cross sections for the reaction $C^+ + H_2 \rightarrow CH^+ + H$ as a function of kinetic energy in the center-of-mass frame (lower *x* axis) and laboratory frame (upper *x* axis). The upper part (offset on the vertical scale) shows guided ion beam data from [77] (small points), the model of Eq. (4) with $n = 1/2$ and $m = 1$ (dashed line), and the convolution of this line over the kinetic energy distributions of the reactants. The lower part shows the guided ion beam data represented by a line along with literature results on uncorrected energy scales for H_2 (solid symbols) and D_2, reaction (5) (open symbols): open triangle, reduced by 35% from Maier [72]; closed square, reduced by 42% from Fennelly [80]; open and closed diamond, Lindemann et al. [78]; closed circle, Frees et al. [79]. Reprinted from [77] with permission.

Fig. 6, in which the absolute energy scale is determined using retarding techniques and verified by time-of-flight methods. Also shown are data from the literature, including that of Maier [72], Koski and co-workers [78,79], and Fennelly [80], all on uncorrected energy scales. Similarly to Maier, Fennelly had "corrected" his energy scale by 0.25 eV, and even though Koski and co-workers accounted for Doppler broadening in their analysis of this system, they too suggested that their energy scale needed to be shifted by about 0.15 eV. Except for the early work of Koski and co-workers, all the "uncorrected" data have the same dependence on kinetic energy and differ acceptably in absolute magnitude. We interpreted the data in the threshold region using Eq. (4) with $n = 1/2$ and $m = 1$, a form that can be derived using microscopic reversibility and the long-range ion–induced dipole potential [81], i.e. the endothermic form of the Langevin-Gioumousis-Stevenson collision cross section [35]. This model cross section, with a threshold energy for reaction (5) taken from literature thermochemistry, is then convoluted with thermal motion of the H_2 reactant as outlined by Chantry and with the kinetic energy distribution of the ions following an extension of Chantry's results given by Lifshitz et al. [82]. It can be seen that the data are reproduced nicely

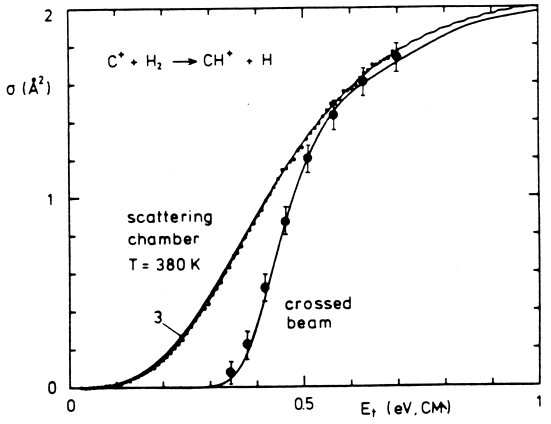

Fig. 7. Cross sections for the reaction $C^+ + H_2 \rightarrow CH^+ + H$ as a function of relative kinetic energy. Small points are taken using a guided ion beam–gas apparatus with the neutral gas at a temperature of 380 K. Large points are taken with crossed neutral-guided ion beam apparatus. The solid lines give cross sections calculated using phase space theory and convoluted appropriately for both experimental cases. Reprinted from [53] with permission.

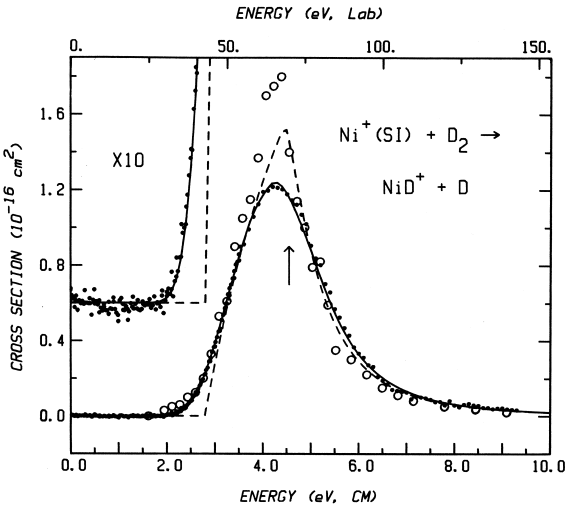

Fig. 8. Cross sections for reaction of Ni^+ (formed by surface ionization, SI) with D_2 as a function of kinetic energy in the center-of-mass frame (lower *x* axis) and laboratory frame (upper *x* axis). The small points show guided ion beam data from [103] and large open circles beam–gas data from [97]. The broken line is the line-of-centers model, Eq. (4) with $n = m = 1$, along with a model for product dissociation above the D_2 bond dissociation energy, 4.55 eV, indicated by the arrow. The full line is this model convoluted with the experimental kinetic energy distributions of the reactants. The inset shows the data and models expanded by a factor of 10 and offset from zero. Reprinted from [103] with permission.

in the threshold region. Later treatments of improved data from our laboratory, including reactions with the H_2, HD, and D_2 isotopic variants, showed that other forms of Eq. (4) (e.g. $n = m$ and $m = 1$) could be used to reproduce the data over a more extended energy range while still keeping the threshold restricted to the known thermochemistry [83]. Further, it was demonstrated that phase space theory accurately describes the relative kinetic energy dependence of this reaction cross section [84,85]. Work on this reaction reached its denouement in the very thorough study of Gerlich et al. [53] in which a supersonic crossed beam of H_2 was used to remove the effects of the kinetic energy distribution of the neutral reactant almost completely, Fig. 7. Further, rotationally state-specific cross sections are derived in this study, and it is shown that nuclear spins are decoupled from the reaction energetics.

Continued work using tandem mass spectrometry in a beam–gas arrangement to study endothermic ion–molecule reactions was pursued by several groups during the 1970s: notably, Koski and co-workers [79,86–88], Futrell and Tiernan [89], and Tiernan and co-workers [82,90–93]. In the early 1980s, Armentrout and Beauchamp began applying such methods to the study of reactions of metal ions, beginning with U^+ [94–96] and then expanding to the transition metal ions, Ni^+ [97] and Co^+ [98,99–101], and several others [102]. An example of this work is shown in Fig. 8, where it can be seen that the data are in good agreement with the much more precise cross sections obtained later by using guided ion beam methods [103]. Murad performed similar work on reactions of alkaline earth metal ions [104,105]. It was this series of articles that caught the attention of those compiling gas phase ion thermochemistry for the first time. In their 1988 review, Lias et al. [106] use the "onsets of endothermic reactions" to acquire several pieces of data, citing several "recent quantitative studies," specifically [87,99,102,105] and references therein.

3.2. Form of the cross section

It should be clear at this point that one of the key problems in interpreting data like those shown in Figs.

6–8 is knowing the energy dependence of the cross section. Unlike ionization phenomena where threshold laws have been derived [107,108], no such rigorous threshold behavior for chemical reactions has been defined. Empirically, two main approaches were developed in early work. Koski used Eq. (6) to model his data, whereas Maier and Tiernan utilized variants of Eq. (4), as noted above for Maier's work. Tiernan's work used $n = 1/2$ and $m = 1$ citing Levine and Bernstein's theoretical work [81]. For collision-induced dissociation, Tiernan and co-workers cited theory of Rebick and Levine [109] to justify using Eq. (4) with $m = 1$ and n an adjustable parameter, usually near 2 for a direct process and between 1.5 and 1.8 for an indirect process. Gerlich has advocated the use of a completely unbiased approach, the use of a polygonal ansatz in which the true cross section is represented by a series of points [53].

In their earliest work, Armentrout and Beauchamp [94] used a linear form of Eq. (4), $n = 1$ and $m = 0$, a result of using the analysis of Chantry directly. Later, these authors [98] discussed appropriate forms for the cross section and chose $n = m$, justifying this form by an appeal to classical expressions for the ratio of numbers of states for a transition state to the density of states for an energized molecule. They also pointed out that this view would allow ready extension to multiple reaction paths, more refined treatments of the number and density of states, and situations where n and m might not be equal.

Aristov and Armentrout [110] examined a variety of theoretical expressions for atom–diatom reactions in the literature. These included $n = m = 0.5$ from scattering theory [111], $n = m = 1$ from the line-of-centers model [112], $n = 1.0$ or 1.25 and $m = 0$ from phase space theory [73,74,113], and the stationary phase approximation yields $n = 2.5$ and $m = 1.5$ for direct processes [114]. Collision theory leads to an expression where $m = 3$ and $n = 3$–4 depending on whether the transition state involved is loose or tight [115]. Results pointing to Eq. (4) with $m = 1$ and $n = 2.5$ [116] or variable [117,118] have been developed by several workers. A recent treatment for collisions of hard ovoids with orientation-dependent energy barriers yields equations more complicated than Eq. (4) but point to $m = 1$ with $n = 2$–4 [119].

An important work in my thinking about this problem comes from Chesnavich and Bowers [120]. Using foundations in transition state theory laid by Marcus [121], these authors derived a form for the cross section of "translationally driven reactions" in which $m = 1$ and $n = 1$–3.5, depending on the properties of the transition state. These latter expressions are particularly appealing because they are specific to cases where the reaction of interest is made possible by kinetic energy, the situation pertaining to most tandem mass spectrometry experiments. Hence, one uses the standard statistical theory result [122–124] for a rate constant, namely,

$$k(E) = L^{\dagger}N^{\dagger}(E_{tot} - E_0)/h\rho(E) \quad (7)$$

where $L^{\dagger}$ is the statistical factor describing the number of equivalent reaction pathways, $N^{\dagger}(E_{\mathrm{tot}} - E_0)$ is the sum of states at the transition state, E_{tot} is the total energy available to the reaction at a kinetic energy E, and $\rho(E)$ is the density of states of the reactants. Because the reaction is driven by the translation energy of the reactants, the density of states used in the denominator is simply the translational density of states, which varies as the reactant velocity, i.e. $E^{1/2}$. To obtain a cross section, the microcanonical rate constant is divided by the velocity, see Eq. (2). This operation gives an expression in which the denominator depends linearly on E, i.e. equivalent to Eq. (4) with $m = 1$. The other degrees of freedom of the molecule are actually included in the expression for $N^{\dagger}(E_{\mathrm{tot}} - E_0)$ which varies as $(E_{\mathrm{tot}} - E_0)^{(\Delta v+2)/2}$, where Δv is the number of vibrational degrees of freedom created upon formation of the transition state. Hence, contributions from many of the other degrees of freedom have essentially canceled. For structureless particles (hard spheres), Δv will be zero and the line-of-centers cross section is recaptured, as it should be.

For several years, my group analyzed our data using Eq. (4) with m of 0, 1, 1.5, 3, and n while allowing n to vary freely. We generally found that our experimental cross sections could be reproduced with

any of these models after convolution over the kinetic energy distributions of the reactants. For atom–diatom reactions, n was often found to lie close to unity, whereas for reactions of atomic metal ions with larger molecules, larger values of n were required. The values of E_0 obtained by these procedures were not sensitive to the choice of m. We have shown explicitly that Eq. (4) with $m = 1$ is better than a linear model, $n = 1$ and $m = 0$ [125]. On the basis of these empirical observations and the theory of Chesnavich and Bowers, our present work uses Eq. (4) with $m = 1$ and n allowed to vary freely to best fit the data after convolution with the kinetic energy distributions and several other effects discussed in the following.

Recent studies have indicated that Eq. (4) with $m = 1$ fails under certain interesting conditions. For instance, Armentrout and co-workers [126,127] and others [128] have shown that when a reaction is limited by coupling between reaction surfaces of different spin, an additional $E^{-1/2}$ factor needs to be introduced such that m is effectively 1.5. As discussed in detail in our most recent work, this expression can be justified by appealing to a Landau-Zener model [129] and agrees with several modern theoretical treatments [130,131] for the kinetic energy dependence of the crossing probability between diabatic surfaces of different spin multiplicities. This experimental work comprises a direct measure of these theoretical predictions.

3.3. High energy behavior

In my earliest work on the kinetic energy dependence of bimolecular ion–molecule reactions [94], I found one experimental observation to be a clear indication that all of the energy in the center of mass frame energy was available to the reactants. As shown in Fig. 8, the cross sections for simple atom–diatom exchange reactions

$$M^+ + AB \rightarrow MA^+ + B \quad (8)$$

reach a maximum at an energy very close to that of the AB bond energy, 4.55 eV for D_2 of Fig. 8. This observation can be explained by noting that

$$M^+ + AB \rightarrow M^+ + A + B \quad (9)$$

equivalent to dissociation of the MA^+ product, becomes thermodynamically accessible at this energy. For the example shown, the maximum cross section lies at a laboratory frame energy of about 70 eV. This comparison unambiguously shows that the raw data must be converted from laboratory energies to the center-of-mass scale using $E(\mathrm{CM}) = E(\mathrm{lab})\ M_N/(M_N + M_I)$, where M_N and M_I are the masses of the neutral and ionic reactant, respectively. Further, as for the data in Fig. 8, the maximum in many cases is located promptly at the thermodynamic threshold, indicating that all of the energy is available to the reaction. This is a key conclusion as it also means that *the threshold for reaction (8) can be expected to occur at the thermodynamic threshold* unless there are specific constraints along the potential energy surface. Because of the attractive long-range interactions of ions and molecules, activation barriers in excess of the endothermicity of a reaction are often absent for ion–molecule reactions [125,132].

Armentrout and Beauchamp [98] introduced a simple means of including the effects of reaction (9) in their data analysis. This model relied on the observation that a power law could describe the behavior of the cross sections at high energies. They also developed [133] a more complicated model based on the sequential impulse model of Mahan et al. [134]. The simple model was refined by Weber et al. [135] to include angular momentum constraints using a treatment for product translational energy distributions outlined by Safron et al. [136]. This latter model is incorporated in the analysis of the data shown in Fig. 8. It can be noted that the onset of reaction (9) equals the expected D_2 bond energy, 4.55 eV, and is not an adjustable parameter in the modeling of the cross section shown.

3.4. Effects of internal energy

Early studies recognized that internally excited reactants would exhibit lower reaction thresholds than ions formed more carefully in their ground state [70,89,137–140]. Beauchamp and I did not confront

this issue in our early studies because this work utilized a surface ionization source of atomic metal ions [94–102], such that only low energy (<0.2 eV) electronic states could be formed. However, my first article as an assistant professor [141] had to deal with this issue head on. Our cross sections for collision-induced dissociation of Mn_2^+ showed a marked dependence on the electron energy used to ionize the $Mn_2(CO)_{10}$ precursor. We soon learned to manipulate our ion sources in controlled ways such that cross sections taken under different ion source conditions could be combined to extract state-specific reaction cross sections of the electronic states of atomic transition metal ions [46,142–145] and of spin-orbit states of rare gas ions [146,147]. (Other state-specific studies using multiphoton [148,149] and photoionization [42] methods to generate such ions have also been pursued.) In our work, these assignments relied on the observation that thresholds would generally shift by the electronic excitation energy, E_{el}, i.e. Eq. (4) is modified to

$$\sigma(E) = \sigma_0(E + E_{el} - E_0)^n/E^m \quad (10)$$

Interestingly, not all electronic states behave in this sensible fashion, but the reasons for such deviant behavior can be understood [46,103].

Whereas the relatively large excitation energies associated with electronic states are readily apparent as shifts in the thresholds of ion–molecule reactions, effects of the much smaller rotational and vibrational energies are less obvious. There are several guided ion beam studies that have demonstrated that rotational energy is available to help drive bimolecular reactions [53,55,150–152], although counterexamples also exist [40,153]. Because of the small amounts of rotational energy available in any reaction system ($3kT/2 = 0.04$ eV at 300 K), definitive experiments are difficult. In contrast, the ability of vibrational energy to lower reaction thresholds is well established, dating from early studies of Chupka on the reactions of $H_2^+(v) + Rg \rightarrow RgH^+ + H$ (Rg = He, Ne) [154]. Guided ion beam studies demonstrating this effect include the $H_2^+(v) + He$ reaction [155], $H_2^+(v) + Ar \rightarrow Ar^+ + H_2$ [42,156], $OCS^+(v) + C_2H_2 \rightarrow OCS + C_2H_2^+$ [44,157], and $C_2H_2^+(v) + CH_4 \rightarrow C_2H_3^+ + CH_3$ [158].

Such beautifully detailed state-specific studies are convincing evidence that the internal energies of ions must be included when the thresholds of endothermic reactions are measured. Therefore, determination of accurate thresholds necessitates careful experimental control of the formation of the reagents and including this available energy in the cross section form used to analyze the data. When a single state is involved in the reaction, it is straightforward to use Eq. (10) where E_{el} can now represent any internal state of the reactants. However, as molecules get more complex, the numbers of ro-vibrational and electronic states can increase rapidly such that an explicit summation over all internal states is needed,

$$\sigma(E) = \sigma_0 \sum g_i(E + E_i - E_0)^n/E^m \quad (11)$$

Here, the states are indexed by i and have energies E_i and relative populations g_i, where $\Sigma g_i = 1$. The need for Eq. (11) was first recognized by Schultz et al. [159] in their study of the collision-induced dissociation (CID) of $Fe(CO)_x^+$ ($x = 1$–5) complexes. What is not intuitive in this approach is the fact that the distribution included by the summation over internal energies introduces substantial curvature into the model cross section. Hence, analysis of the data using Eq. (10) where E_{el} equals the average internal energy yields a different threshold energy, E_0, than analysis with Eq. (11). This conclusion is illustrated in Fig. 9 [125] for the CID of $Fe(CO)_5^+$ that had been carefully thermalized in a flow tube ion source [160]. Analysis of the data using Eq. (10) with $E_{el} = 0.28$ eV (the average internal energy of room temperature $Fe(CO)_5^+$ ions) yielded $E_0 = 1.07 \pm 0.06$ eV, whereas analysis with Eq. (11) gave 1.16 ± 0.04 eV. As shown in Fig. 9, the reason for this difference is that a larger value of the parameter n is needed to reproduce the data when Eq. (10) is used. The additional curvature introduced by the internal energy distribution allows very accurate reproduction of the data using a lower value of n with Eq. (11). (Although this approach seems obvious in retrospect, it is interesting to note that we did not publish these CID data

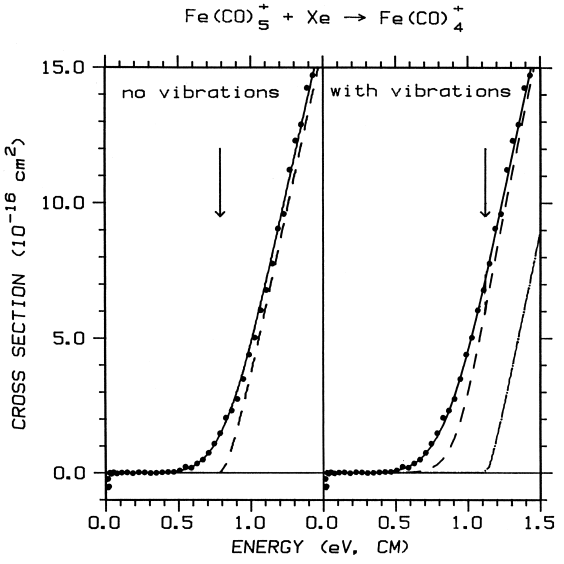

Fig. 9. Collision-induced dissociation cross sections of $Fe(CO)_5^+$ with Xe as a function of kinetic energy in the center-of mass frame. To the left, the dashed line is the model of Eq. (10) with $E_0 = 1.07$ eV and $E_{el} = 0.28$ eV such that the effective threshold is at 0.79 eV (indicated by the arrow). To the right, the dashed line is the model of Eq. (11) with $E_0 = 1.16$ eV that explicitly includes the distribution of internal energies of the ions at 300 K. The dash-dot line shows this model for reactants with an internal temperature of 0 K. In both parts, the full lines are the models convoluted over the experimental kinetic energy distributions of the reactants. Reprinted from [125] with permission.

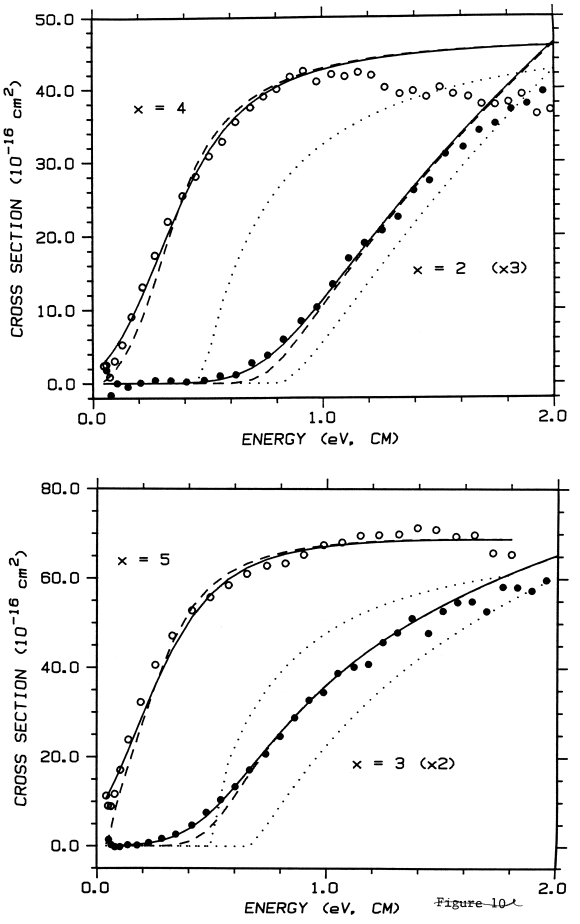

Fig. 10. Collision-induced dissociation cross sections of $H_3O^+(H_2O)_x$ clusters with Xe as a function of kinetic energy in the center-of-mass frame. Dashed lines show the models of Eq. (11) that explicitly includes the distribution of internal energies of the ions at 300 K. Full lines are these models convoluted over the experimental kinetic energy distributions of the reactants. Dotted lines show these models for reactants with an internal temperature of 0 K. Reprinted from [161] with permission.

for over 1.5 years before realizing that accurate thermochemistry could not be obtained without this explicit handling of the internal energies.)

The accuracy of using Eq. (11) was tested to some degree in the $Fe(CO)_x^+$ study by comparing the sum of the five bond energies ($x = 1$–5) with that calculated from literature heats of formation for Fe^+, CO, and $Fe(CO)_5^+$. A much more stringent test of this approach came in the form of CID studies of proton-bound water clusters, $H_3O^+(H_2O)_x$ where $x = 1$–5 [161]. These are systems for which thermochemistry is available from several equilibrium studies, most notably from Kebarle and co-workers [162,163] and Meot-Ner and Speller [164]. CID data for carefully thermalized clusters are shown in Fig. 10, which shows analyses performed using Eq. (11). It can be seen that the apparent thresholds are well below the E_0 values indicated by the onsets of the dotted lines. The data were also analyzed by using Eqs. (4) and (10). The thresholds derived from each of these methods were compared with the literature values. These comparisons show fairly conclusively that Eq. (11) provides the best agreement for all clusters with mean absolute deviations of 3.0 ± 1.9 kJ/mol from Kebarle's work and 4.4 ± 1.4 kJ/mol from the values of Meot-Ner and Speller. Considering that the absolute errors are 6 and 4 kJ/mol in our CID values and those from the equilibrium studies, respectively, these

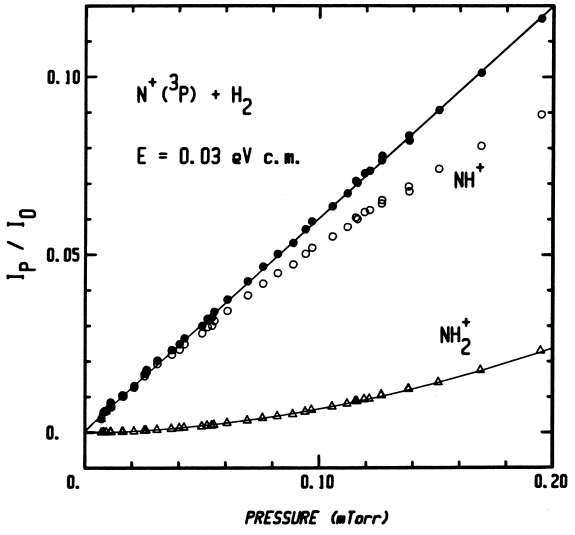

Fig. 11. Ratio of product ion intensity to incident ion intensity as a function of the H_2 neutral reactant gas pressure for the reaction shown at a center-of-mass energy of 0.03 eV. The solid circles are the sum of all product ion intensities. Lines indicate a linear and quadratic fit to the data for the total product ion intensity and the NH_2^+ product ion intensity, respectively. Reprinted from [167] with permission.

deviations indicate excellent agreement. These results demonstrate unambiguously that the internal energy of the clusters is available to induce dissociation.

3.5. Effects of multiple collisions

In any tandem mass spectrometer, there is always the possibility that the reactant ion can undergo more than one collision with the neutral reagent (or that a product of the first collision can undergo a collision with the neutral). Such processes have been known and understood for 30 years [165,166]. For most early tandem mass spectrometry experiments, the effects of such additional collisions were small, in part because signals were sufficiently low that the experiments were not particularly sensitive to these effects. With the enhanced sensitivity afforded by guided ion beams, it was straightforward to observe such processes [35,23,167] and demonstrate that they could be characterized by their pressure dependence. Fig. 11 shows an example of this pressure dependence for the $N^+ + H_2$ reaction system. Here, formation of NH_2^+ is observed to have a quadratic dependence on pressure, indicating it is formed in the secondary process, $NH^+ + H_2 \rightarrow NH_2^+ + H$. Because it is impossible to completely remove the effects of secondary collisions using experimental methods, cross sections corresponding to single-collision conditions could be acquired by linearly extrapolating to zero pressure or by adding the cross sections for the secondary products to those of the primary product, Fig. 11.

In bimolecular reactions, the effects of pressure are observed most readily at low energies for sequential exothermic processes because such reactions are efficient and the reactant and product ions spend more time in the collision cell. In general, bimolecular reactions that are endothermic are not particularly sensitive to the neutral pressure largely because the transient intermediate complexes involved are short lived and unlikely to collide with another neutral reactant during their lifetime. However, collision-induced dissociation reactions, which are intrinsically endothermic, show a pronounced dependence on pressure. We first realized this in a study of the CID of niobium cluster cations [168] and shortly thereafter for the $Fe(CO)_x^+$ study [159], showing that it was a general phenomenon. An example of such pressure dependence is shown in Fig. 12, where it can be seen that the apparent thresholds for loss of one and two CO ligands from $Fe(CO)_4^+$ decreases systematically as the pressure of the Xe neutral reagent increases. To a first approximation, two collisions can deposit twice the energy of a single collision such that the thresholds shift down by a factor of 1/2. Hence, the effect is larger for the process having the larger threshold. It should also be realized that for the data shown, the experiments are conducted in what would ordinarily be considered the “single collision” regime. Specifically, the probability that an ion undergoes a single collision at the three pressures shown is approximately 3%, 10%, and 17%. Hence, the probability of a second collision is only about 3% even at the highest pressure shown. This sensitivity to multiple collisions was surprising at first, but is a straightforward consequence of the long lifetime of the collisionally activated molecule and how strongly dependent the unimolecular decomposition probability is on the energy

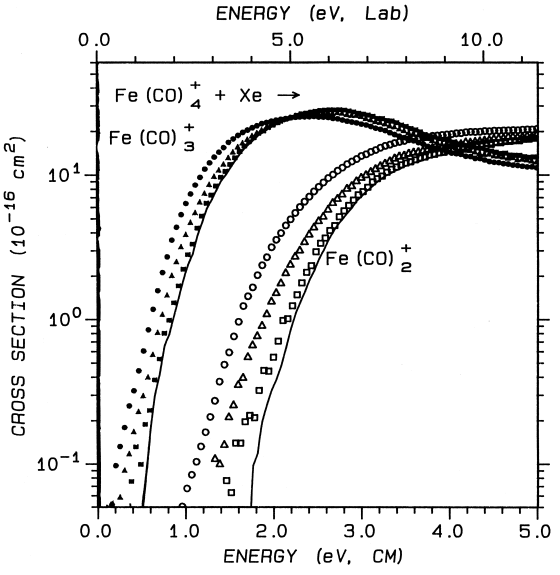

Fig. 12. Collision-induced dissociation cross sections of $Fe(CO)_4^+$ with Xe losing one and two carbonyl ligands as a function of kinetic energy in the center-of mass frame (lower *x* axis) and laboratory frame (upper *x* axis). Circles, triangles, and squares show results obtained at Xe pressures of 0.38, 0.16, and 0.04 mTorr, respectively. The solid lines show the linear extrapolations of these cross sections to zero pressure. Reprinted from [159] with permission.

of the dissociating species near threshold. Thus, deposition of even a little more energy by a secondary collision can enhance the probability of decomposition by orders of magnitude in the threshold region.

3.6. Collision-induced dissociation

CID has been a mass spectrometric tool for many years. Often, it is used as a qualitative probe of ion structure, conducted at either high (kilovolt) [169,170] or low collision energies [171,172]. The dynamics of CID processes have also been thoroughly studied [173]. However, the use of the CID process to measure thermochemistry of ions is relatively recent, sufficiently so that in their 1990 review of "collision-induced decomposition of ions", Bordas-Nagy and Jennings make no mention of such studies [174].

In my mind, the possibility of using CID to measure accurate thermochemistry was substantiated by the results of Parks and co-workers on the collision-induced ion-pair formation of metal halides [117,175–177]. One of the earliest studies of the CID of molecular ions that hinted at such a use concerned UO^+ and UO_2^+ by Armentrout and Beauchamp [95]. We found dissociation thresholds slightly lower than known U^+-O and OU^+-O bond energies, although in retrospect, it seems likely that the multiple collisions lowered these thresholds. Koski and co-workers [88,178] performed CID studies to determine thermodynamic information in a similar time frame. The first article from my group involved such a study of the Mn_2^+ ion [141]. Other notable studies using CID methods that appeared somewhat later include the observation by Michl and co-workers[179,180] and Marinelli and Squires [181] that a second solvent molecule can bind to a transition metal ion more strongly than the first. This observation, which seems counter to expectations from simple electrostatic considerations, is now well understood in terms of electronic rehybridization at the metal center [51,52,182–184].

Presently, the use of CID as a tool for measuring bond energies is an active area of research. The accuracy of thermodynamic data acquired in such studies depends on several factors already mentioned. Specifically, collision energies should be well defined; the ions of interest must have well-characterized internal energies; cross sections corresponding to single collision conditions should be analyzed; and the analysis should include all sources of energy and their explicit distributions. In addition, several other factors important, but not unique, to CID reactions are outlined in the following sections.

3.7. Effect of collision partner

Aristov and Armentrout [185] made an important observation in their examination of the CID of thermalized VO^+ with the five rare gases, He, Ne, Ar, Kr, and Xe. No dissociation was observed for He, whereas the other four systems yielded CID thresholds consistent with the known V^+-O bond energy. However, the CID efficiency at threshold was clearly highest for Xe, a result that has been verified for other systems [159,186,187]. We believe that Xe is the most efficient collision partner for inducing dissocia-

tion at threshold because Xe is the heaviest and most polarizable of the stable rare gases. These properties allow energy to be transferred from translation to internal degrees of freedom in the most efficient manner possible.

To see why this observation is reasonable, we view a CID as a two-step process: a collisional excitation step,

$$AB^+ + Rg \rightarrow [AB \cdot Rg]^+ \rightarrow AB^{+*} + Rg \qquad (12a)$$

followed by a unimolecular decomposition,

$$AB^{+*} \rightarrow A^+ + B \qquad (12b)$$

Historically, the excitation step reaction (12a) was generally thought of as impulsive [174], however, the relatively strong interaction with the polarizable Xe atom can yield a more statistically behaved $[AB \cdot Rg]^+$ intermediate complex in which energy is randomized. For a statistical decomposition, it is well known that the kinetic energy distribution of the products is sharply peaked close to zero energy [188]. Hence, most of the excitation is left in internal modes of the products of reaction (12a). Because Xe is atomic, this product cannot carry away any of the excess energy in internal degrees of freedom, leaving most of the energy in AB^+. Clearly, this statistical picture can break down depending on the details of the system being studied [189,190]. However, the use of Xe as a collision partner helps assure statistical behavior and this approximation should only get better as the molecular ions get increasingly complex [174].

3.8. Kinetic shift modeling with unimolecular theory

Because the excited AB^{+*} species are moving through the ion beam apparatus on their way to the detector, they have a finite time to decompose. In our guided ion beam instruments, this time is about 10^{-4} s. As the AB^+ molecule becomes larger and more complex, its lifetime for dissociation begins to exceed this time, such that efficient dissociation of the molecule will not be observed at the thermodynamic threshold, but will be delayed until higher energies. (Note that the extra energy imparted by a second collision can change rate of dissociation dramatically.) This so-called "kinetic shift" can appear in any type of threshold measurement [191]. It became obvious to us that explicit consideration of this effect was necessary when we began to examine the CID of transition metal clusters larger than about six atoms [186,192]. M_x^+-M bond energies that were implausibly large were obtained from routine analysis of our CID cross sections with Eq. (11).

The second step of our hypothetical reaction sequence, process (12b), is subject to treatment by modern statistical theories [122–124], such as Rice-Ramsperger-Kassel-Marcus (RRKM) theory. We took advantage of this concept to attempt a quantitative assessment of the kinetic shift in our modeling of the CID behavior of increasingly complex molecules. Our initial treatment [186] was later modified slightly [193] to be conceptually more correct, and recently, has been put on firmer theoretical ground [194]. The treatment yields

$$\sigma(E) = \left(n\sigma_0/E^m\right) \sum_i g_i \int_0^{E+E_i-E_0} \left[1 - e^{-k(E+E_i-\Delta E)\tau}\right] \cdot (\Delta E)^{n-1} d(\Delta E) \qquad (13)$$

an adaptation of Eq. (11) in which ΔE is the energy remaining in relative translational motion after the collision between reactants, the rate constant k is given by Eq. (7), and τ is the time available for dissociation. When the rate constant is fast, the term in square brackets becomes unity, and the integration reverts Eq. (13) back to the empirical form of Eq. (11).

As in any statistical theory for unimolecular decomposition, the calculated rates are highly dependent on the choice of the molecular parameters for the transition state because these control the sum of states in the numerator of Eq. (7). In our recent work [194], we suggested that for many situations of current interest, the transition state is a loose one located at the centrifugal barrier. Hence, it is close to nearly complete dissociation to products, such that the molecular parameters are simply those of the products,

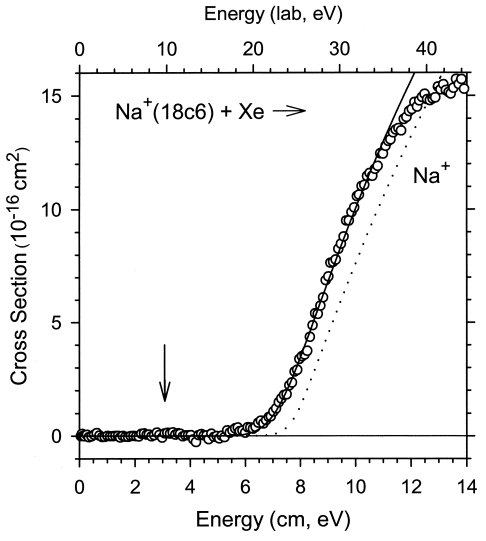

Fig. 13. Collision-induced dissociation cross sections of Na^+(18-crown-6) with Xe as a function of kinetic energy in the center-of mass frame (lower *x* axis) and laboratory frame (upper *x* axis). The dotted line shows the model of Eq. (13) incorporating RRKM modeling in the PSL limit for reactants with an internal temperature of 0 K. The solid line shows this model convoluted with the kinetic and internal energy distributions of the reactants. The arrow indicates the E_0 threshold, 3.07 eV, used in the model shown. Adapted from [198].

making them straightforward to ascertain. This phase space limit (PSL) or orbiting transition state is the loosest transition state possible and provides a rigorous lower limit to the kinetic shift. Application of the PSL in several systems where it is appropriate has yielded reasonable thermochemistry as verified by comparisons with other experiments [195–197] and with ab initio calculations [196–200]. An extreme example, shown in Fig. 13, is Na^+ complexed to the cyclic crown ether, 18-crown-6, c-$(C_2H_4O)_6$ [198]. This molecule is a large floppy ligand with many degrees of freedom. Analysis excluding kinetic shifts yields a threshold for the data shown of 7.37 ± 0.24 eV, comparable to where the dashed line deviates from zero, i.e. the apparent threshold including the considerable internal energy of this molecule at room temperature. If we assume a tight transition state with molecular parameters chosen as those of the complex minus a metal–ligand stretch (an unrealistic assumption), then the threshold moves down to 2.23 ± 0.20 eV. Use of the loose PSL transition state yields the reproduction of the data shown in Fig. 13 and a threshold of 3.07 ± 0.20 eV. High-level ab initio calculations [201] predict a Na^+(18c6) bond energy of 3.44 eV, in agreement with the PSL value within the combined experimental and theoretical uncertainties. Indeed, comparisons of many different alkali metal ion complexes with mono-, bi-, and polydentate ethers, most of which have negligible or small kinetic shifts, indicate theory at this level is systematically higher than our experimental results by 12 ± 8% [196]. This is certainly a promising result and bodes well for continued application of the model of Eq. (13) given judicious choices of the transition state parameters. It might also be mentioned that although most of the applications of the kinetic shift modeling in our group have involved CID processes, consideration of such effects should also be important for bimolecular reactions involving complex molecules.

The largest remaining uncertainty in the modeling of CID processes is the distribution of excitation energies deposited in the AB^+ molecule in reaction (12a). In our present model, this distribution is included empirically by the parameter *n* in Eq. (13). Efforts in our laboratory are underway to measure this energy deposition distribution explicitly in several cases so that more precise models can be developed.

3.9. Competitive shifts

Eq. (13) considers only a single channel of reaction or decomposition. If there are more channels, indexed here by *j*, each having separate thresholds, $E_{0,j}$, then there is a straightforward means of incorporating the competition between these channels in a statistical way. Specifically, Rodgers and Armentrout [202] noted that the total rate of dissociation (or reaction) is given by unimolecular theory as

$$k_{tot}(E^*) = \sum_j k_j(E^*) = \sum_j L^{\dagger} N_j^{\dagger}(E^* - E_{0,j})/h\rho(E^*) \quad (14)$$

where $E^* = E + E_i - \Delta E$ is the excitation energy of the molecule. The total cross section for dissociation

(or reaction) is divided among the channels such that $\sigma_j = (k_j/k_{tot})\,\sigma_{tot}$. However, this ratio of rates must be included in the integration over the excitation energy in Eq. (13) leading to

$$\sigma_j(E) = (n\sigma_{0,j}/E^m) \sum_i g_i \int_0^{E+E_i-E_0} [k_j(E^*)/k_{tot}(E^*)] \cdot [1 - e^{-k_{tot}(E^*)\tau}](\Delta E)^{n-1} d(\Delta E) \quad (15)$$

This expression includes no new adjustable parameters other than the thresholds for each new channel. The shape of the total reaction cross section is governed by parameter n for all channels, properly reflecting the competition among channels. Because multiple channels need to be reproduced simultaneously, the fitting of the data is much more constrained. Nevertheless, excellent results have been obtained, not only in the original work on the dissociation of $Li^+(ROH)(R'OH)$ complexes [202] but in several articles of other researchers. These include studies of gas phase acidities [203,204], proton affinities [205], hydronium ion affinities [206], and metal cluster dissociation energies [207,208]. Fig. 14 shows the example of the proton bound dimer of HC_4^- and $^-CH_2CHO$ [204]. The observation that the two cross sections intersect indicates that the transition states for the two channels differ appreciably, a finding consistent with ab initio calculations. The modeling shown uses transition state parameters obtained from these calculations. The difference in the two thresholds, 18 ± 3 kJ/mol, equals the relative gas-phase acidity of diacetylene and acetaldehyde. This relative acidity can be combined with the electron affinity of C_4H to yield a HC_4-H bond energy of 539 ± 12 kJ/mol, comparable to the HC_2-H bond energy of acetylene, 551.2 ± 0.1 kJ/mol [209].

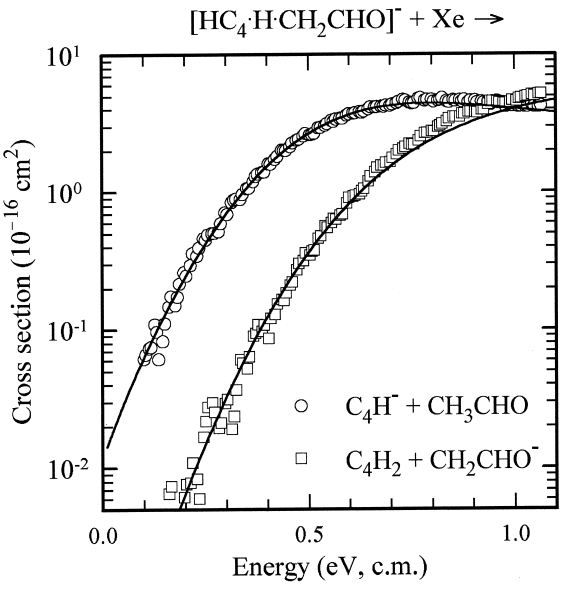

Fig. 14. Competitive collision-induced dissociation cross sections of C_4H^-(acetaldehyde) complexes as a function of kinetic energy in the center-of mass frame. Solid lines are the models using RRKM theory, Eq. (15), to calculate the product branching ratio as a function of available energy, as convoluted with the kinetic and internal energy distributions of the reactants. Reprinted from [204] with permission.

4. Conclusion and prospects

Although the use of rf ion guides has developed slowly since their introduction in 1974, applications of these devices has burgeoned in the past few years. Their properties make them ideal for the guided ion beam tandem mass spectrometry experiments detailed in this review. In this more limited area, active work is restricted to only about a dozen groups, although this number has gradually increased over the years. Certainly, the development of ion guides has permitted kinetic energy dependent integral cross sections of extremely high quality to be obtained routinely. Such high quality data has demanded quantitative explanation and modeling.

In spite of the lack of a rigorous threshold law for cross sections of chemical reactions, the use of tandem mass spectrometry to measure thermodynamic information has reached the potential originally envisioned by Giese and Maier [69]. The use of the empirical expressions, Eq. (4) and its variants, Eqs. (11), (13), and (15), to reproduce the energy dependence of cross sections has proven to be robust and to yield accurate thermochemistry within the uncertainties of the determinations for many systems

[48,51,52,125]. The uncertainties can vary widely and are highly dependent on the system under examination. They have ranged from as small as 3 meV for the slightly endothermic (by 11 meV) $N^+ + H_2$ reaction [55], to more typical values of about ±0.04 eV for atom–diatom reactions, to an order of magnitude larger for reactions of complex species. It seems likely that more general applications of phase space theory, successfully applied to a few small systems [40,53,55,85,150,210–212], may provide less empirical approaches to modeling threshold behavior.

Despite the successes achieved, threshold measurements are not a panacea. To obtain accurate thermochemistry, the experimental conditions must be controlled and the cross sections analyzed with care. The variety of considerations that are involved, outlined above, must all be included or judiciously excluded. Even then, there are always going to be surprises. (1) The reaction observed may have a barrier along the reaction pathway in excess of the endothermicity [102,211,212]. (2) The dynamic behavior of the reaction of interest may not conform to the simple formulas, Eqs. (4) and others, now routinely applied. For instance, we have found that the measurement of the bond energies of strongly bound small molecules is difficult using CID methods [185,213–215], probably because coupling between the translational and internal degrees of freedom is inefficient at such high thresholds. Several other examples of systems that exhibit nonthermodynamic behavior have been discussed previously [125]. Among our more recent results is the interesting case of CID of the $Li^+(H_2O)$ complex by rare gas atoms, Rg [189]. This system shows evidence for strong contributions from indirect pathways, i.e. formation of $LiRg^+$ followed by dissociation to Li^+. (3) The models may begin to fail or become inaccurate as the size of the system gets larger. Our results for M^+(18c6) complexes are encouraging [198], especially when it is remembered that this degree of accuracy on such a complex system could not have been accomplished even five years ago. Nevertheless, the extrapolation needed to get from the apparent threshold to the "real" threshold is substantial (over a factor of 2), Fig. 13. Accurate input data, in terms of the molecular parameters for the transition state and the energized molecule, become increasingly critical components of the analysis and inaccuracies in these values can lead to appreciable errors in the resultant thresholds. Honest error assessments will be crucial in such applications. Largely because such issues can now be identified, this author is optimistic that guided ion beam tandem mass spectrometry has not yet reached its full potential.

Acknowledgements

Our guided ion beam mass spectrometer studies of ion kinetics, dynamics, and thermochemistry have been supported over the years by the National Science Foundation and the Department of Energy, among others. The work has been the beneficiary of the insight, hard work, and dedication of a great group of students and postdocs, whom I thank profusely. I also want to thank my present colleague, Professor Scott Anderson, for helping to introduce me to rf ion guides when he was a graduate student and I was a beginning assistant professor and to Professor Kent Ervin for helpful comments on the manuscript.

References

[1] H.M. Rosenstock, K. Draxl, B.W. Steiner, J.T. Herron, J. Phys. Chem. Ref. Data 6 (1977) Suppl. 1, 1.
[2] D. Gerlich, Diplomarbeit, University of Freiburg, Federal Republic of Germany, 1971.
[3] E. Teloy, D. Gerlich, Chem. Phys. 4 (1974) 417.
[4] S.G. Lias, J.E. Bartmess, in Gas-Phase Ion Thermochemistry in NIST Chemistry WebBook, NIST Standard Reference Database Number 69, W.G. Mallard, P.J. Linstrom (Eds.), National Institute of Standards and Technology, Gaithersburg, MD, 2000 (http://webbook.nist.gov).
[5] M. Henchman, in Ion–molecule Reactions, J.L. Franklin (Ed.), Plenum, New York, 1972, Vol. 1, p. 101.
[6] W.R. Gentry, in Gas Phase Ion Chemistry, M.T. Bowers (Ed.), Academic, New York, 1979, Vol. 2, p.221.
[7] J.M. Farrar, in Techniques for the Study of Ion–molecule Reactions, J. M. Farrar, W. H. Saunders (Eds.), Wiley, New York, 1988, p. 325.
[8] G. Ochs, E. Teloy, J. Chem. Phys. 61 (1974) 4930.
[9] W. Frobin, Ch. Schlier, K. Strein, E. Teloy, J. Chem. Phys. 67 (1977) 5505.
[10] S.M. Trujillo, R.H. Neynaber, E.W. Rothe, Rev. Sci. Instrum. 37 (1966) 1655.

[11] W.R. Gentry, D.J. McClure, C.H. Douglass, Rev. Sci. Instrum. 46 (1975) 367.
[12] D. Gerlich, Adv. Chem. Phys. 82 (1992) 1.
[13] H. Villinger, J.H. Futrell, A. Saxer, R. Richter, W. Lindinger, J. Chem. Phys. 80 (1984) 2543.
[14] M.T. Rodgers, S. Campbell, E.M. Marzluff, J.L. Beauchamp, Int. J. Mass Spectrom. Ion Processes 137 (1994) 121.
[15] Y. Wang, S.D.-H. Shi, C.L. Hendrickson, A.G. Marshall, Int. J. Mass Spectrom. 198 (2000) 113, and references therein.
[16] R.A. Yost, C.B. Enke, Anal. Chem. 51 (1979) 1251.
[17] M. Okumura, L.I. Yeh, Y.T. Lee, J. Chem. Phys. 83 (1985) 3705.
[18] M.F. Jarrold, K.M. Creegan, Int. J. Mass Spectrom. Ion Processes 102 (1990) 161.
[19] J.P. Maier, Mass Spectrom. Rev. 11 (1992) 119.
[20] Y. Shi, V.A. Spasov, K.M. Ervin, J. Chem. Phys. 111(1999) 938.
[21] L.D. Landau, E.M. Lifshitz, Mechanics, 3rd ed., Oxford, New York, 1976.
[22] Z. Herman, R. Wolfgang, in Ion–molecule Reactions, J.L. Franklin (Ed.), Plenum, New York, 1972, Vol. 2, p. 553.
[23] K.M. Ervin, P.B. Armentrout, J. Chem. Phys. 83 (1985) 166.
[24] D. Gerlich, in XVIII. International Conference on Physics of Electronic and Atomic Collisions, T. Andersen, B. Fastrup, F. Folkmann, H. Knudsen (Eds.), AIP, New York, 1993, p. 607.
[25] P. Tosi, F. Eccher, D. Bassi, F. Pirani, D. Cappelletti, V. Aquilanti, Phys. Rev. Lett. 67 (1991) 1254.
[26] W. Lindinger, E. Alger, H. Störi, M. Pahl, R.N. Varney, J. Chem. Phys. 67 (1977) 3495.
[27] I. Dotan, W. Lindinger, J. Chem. Phys. 76 (1982) 4972.
[28] S. Rosin, I.I. Rabi, Phys. Rev. 48 (1935) 373.
[29] I. Amdur, J.E. Jordon, Adv. Chem. Phys. 10 (1966) 29.
[30] A. Henglein, K. Lacmann, B. Knoll, J. Chem. Phys. 43 (1965) 1048.
[31] A. Henglein, K. Lacmann, G. Jacobs, Ber. Bunsenges Phys. Chem. 69 (1965) 279; 69 (1965) 286.
[32] J.B. Homer, R.S. Lehrle, J.C. Robb, D.W. Thomas, Adv. Mass Spectrom. 3 (1966) 415.
[33] D. Hyatt, K. Lacmann, Z. Naturforsch. Teil A 23 (1968) 2080.
[34] K. Tanaka, J. Dirup, T. Kato, I. Koyano, J. Chem. Phys. 74 (1981) 5561.
[35] P. Langevin, Ann. Chem. Phys. 5 (1905) 245.
[36] G. Gioumousis, D.P. Stevenson, J. Chem. Phys. 29 (1958) 294.
[37] J.D. Burley, K.M. Ervin, P.B. Armentrout, Int. J. Mass Spectrom. Ion Processes 80 (1987) 153.
[38] E. Haufler, S. Schlemmer, D. Gerlich, J. Phys. Chem. 101 (1997) 6441.
[39] V.F. DeTuri, P.A. Hintz, K.M. Ervin, J. Phys. Chem. A 101 (1997) 5969.
[40] K. Rempala, K.M. Ervin, J. Chem. Phys. 112 (2000) 4579.
[41] K. Do, T.P. Klein, C.A. Pommerening, L.S. Sunderlin, J. Am. Soc. Mass Spectrom. 8 (1997) 688.
[42] C.-Y. Ng, Adv. Chem. Phys. 82 (1992) 401.
[43] S.L. Anderson, F.A. Houle, D. Gerlich, Y.T. Lee, J Chem. Phys. 75 (1981) 2153; F.A. Houle, S.L. Anderson, D. Gerlich, T. Turner, Y.T. Lee, ibid. 77 (1982) 748.
[44] S.L. Anderson, Adv. Chem. Phys. 82 (1992) 177.
[45] L.A. Posey, R.D. Guettler, N.J. Kirchner, R.N. Zare, J. Chem. Phys. 101 (1994) 3772.
[46] P.B. Armentrout, Annu. Rev. Phys. Chem. 41 (1990) 313.
[47] D.C. Parent, S.L. Anderson, Chem. Rev. 92 (1992) 1541.
[48] P.B. Armentrout, D.A. Hales, L. Lian, in Advances in Metal and Semiconductor Clusters, M.A. Duncan (Ed.), JAI, Greenwich, CT, 1994, Vol. 2, p. 1.
[49] S. Nonose, H. Tanaka, T. Mizuno, J. Hirokawa, T. Kondow, J. Chem. Phys. 104 (1996) 5869; S. Nonose, H. Tanaka, T. Mizuno, N. J. Kim, K. Someda, T. Kondow, ibid. 105 (1996) 9167; H. Tanaka, T. Mizuno, F. Ishizaki, S. Nonose, T. Kondow, ibid. 106 (1997) 4002.
[50] Y. Shi, V.A. Spasov, K.M. Ervin, J. Chem. Phys. 111 (1999) 938; V.A. Spasov, T.H. Lee, J.P. Maberry, K.M. Ervin, ibid. 110 (1999) 5208.
[51] P.B. Armentrout, B.L. Kickel, in Organometallic Ion Chemistry, B.S. Freiser (Ed.), Kluwer, Dordrecht, 1996, p. 1.
[52] M.T. Rodgers, P.B. Armentrout, Mass Spectrom. Rev., 19 (2000) 215.
[53] D. Gerlich, R. Disch, S. Scherbarth, J. Chem. Phys. 87 (1987) 350.
[54] P. Tosi, O. Dmitriev, D. Bassi, J. Chem. Phys. 97 (1992) 3333.
[55] P. Tosi, O. Dmitriev, D. Bassi, O. Wick, D. Gerlich, J. Chem. Phys. 100 (1994) 4300.
[56] D J. Levandier, R.A. Dressler, S. Williams, E. Murad, J. Chem. Soc., Faraday Trans. 93 (1997) 2611.
[57] D.J. Levandier, R.A. Dressler, E. Murad, Rev. Sci. Instrum. 68 (1997) 64.
[58] O. Sublemontier, L. Poisson, P. Pradel, J.M. Mestdagh, J.P. Visticot, J. Am. Soc. Mass Spectrom. 22 (2000) 160.
[59] W.J. Knott, D. Proch, K.L. Kompa, Ch. Rose-Petruck, J. Chem. Phys. 201 (1995) 214.
[60] O. Dutuit, H. Palm, D. Berthomieu, Z. Herman, Chem. Phys. 209 (1996) 259.
[61] Other instruments incorporating guided ion beams as defined here include those of P. Hierl (U. Kansas), M.T. Rodgers (Wayne State U.), R.R. Squire, H. Kenttamaa (Purdue U.), C. Wesdemiotis (Akron U.).
[62] J. H. Futrell, Adv. Chem. Phys. 82 (1992) 401.
[63] S. Mark, D. Gerlich, Chem. Phys. 209 (1996) 235.
[64] S.L. Anderson, Acc. Chem. Res. 30 (1997) 28.
[65] M.J. Bastian, R.A. Dressler, E. Murad, J. Chem. Phys. 103 (1995) 144.
[66] F. Muntean, P.B. Armentrout, unpublished.
[67] Y.-H Chiu, H. Fu, J.-T. Huang, S.L. Anderson, J. Chem. Phys. 105 (1996) 3089.
[68] S. Williams, Y.-H. Chiu, D.J. Levandier, R.A. Dressler, J. Chem. Phys. 109 (1998) 7450.
[69] C.F. Giese, W.B. Maier, J. Chem. Phys. 39 (1963) 197.
[70] W.B. Maier, J. Chem. Phys. 41 (1964) 2174.
[71] W.B. Maier, J. Chem. Phys. 42 (1965) 1790.
[72] W.B. Maier, J. Chem. Phys. 46 (1967) 4991.
[73] J.C. Light, J. Chem. Phys. 40 (1964) 3221.
[74] P. Pechukas, J.C. Light, J. Chem. Phys. 42 (1965) 3281.

[75] P.J. Chantry, J. Chem. Phys. 55 (1971) 2746.
[76] D.G. Truhlar, J. Chem. Phys. 51 (1969) 4617.
[77] K.M. Ervin, P.B. Armentrout, J. Chem. Phys. 80 (1984) 2978.
[78] E. Lindemann, L.C. Frees, R.W. Rozette, W.S. Koski, J. Chem. Phys. 56 (1972) 1003.
[79] L.C. Frees, P.L. Pearl, W.S. Koski, Chem. Phys. Lett. 63 (1979) 108.
[80] P.F. Fennelly, Ph.D. thesis, Brandeis University, 1972 (University Microfilms, Ann Arbor, MI, No. 72-32095).
[81] R.D. Levine, R.B. Bernstein, J. Chem. Phys. 56 (1972) 2281.
[82] C. Lifshitz, R.L.C. Wu, T.O. Tiernan, D.T. Terwilliger, J. Chem. Phys. 68 (1978) 247.
[83] K.M. Ervin, P.B. Armentrout, J. Chem. Phys. 84 (1986) 6738.
[84] W.J. Chesnavich, V.E. Akin, D.A. Webb, Astrophys. J. 287 (1984) 676.
[85] K. M. Ervin, P. B. Armentrout, J. Chem. Phys. 84 (1986) 6750.
[86] R.J. Cotter, R.W. Rozett, W.S. Koski, J. Chem. Phys. 57 (1972) 4100.
[87] W.S. Koski, in Interactions Between Ions and Molecules, P. Ausloos (Ed.), Plenum, New York, 1975, p. 215.
[88] H.P. Watkins, W.S. Koski, Chem. Phys. Lett. 77 (1981) 470.
[89] J.H. Futrell, T.O. Tiernan, in Ion–molecule Reactions, J.L. Franklin (Ed.), Plenum, New York, 1972, Vol. 2, p. 485.
[90] T.O. Tiernan, B.M. Hughes, C. Lifshitz, J. Chem. Phys. 55 (1971) 5692.
[91] C. Lifshitz, R.L.C. Wu, T.O. Tiernan, J. Am. Chem. Soc. 100 (1978) 2040.
[92] T.O. Tiernan, R.L.C. Wu, Adv. Mass Spectrom. 7A (1978) 136.
[93] R.L.C. Wu, T.O. Tiernan, Planet. Space Sci. 29 (1981) 735.
[94] P.B. Armentrout, R.V. Hodges, J.L. Beauchamp, J. Chem. Phys. 66 (1977) 4683.
[95] P.B. Armentrout, J.L. Beauchamp, Chem. Phys. 50 (1980) 21, 27.
[96] P.B. Armentrout, J.L. Beauchamp, J. Phys. Chem. 85 (1981) 4103.
[97] P.B. Armentrout, J.L. Beauchamp, Chem. Phys. 50 (1980) 37.
[98] P.B. Armentrout, J.L. Beauchamp, J. Chem. Phys. 74 (1981) 2819.
[99] P.B. Armentrout, J.L. Beauchamp, J. Am. Chem. Soc. 103 (1981) 784.
[100] P.B. Armentrout, L.F. Halle, J.L. Beauchamp, J. Am. Chem. Soc. 103 (1981) 6624.
[101] P.B. Armentrout, J.L. Beauchamp, J. Am. Chem. Soc. 103 (1981) 6628.
[102] P.B. Armentrout, L.F. Halle, J.L. Beauchamp, J. Chem. Phys. 76 (1982) 2449.
[103] J.L. Elkind, P.B. Armentrout, J. Phys. Chem. 90 (1986) 6576.
[104] E. Murad, J. Chem. Phys. 75 (1981) 4080.
[105] E. Murad, J. Chem. Phys. 78 (1983) 6611.
[106] S.G. Lias, J.E. Bartmess, J.F. Liebman, J.L. Holmes, R.D. Levin, W.G. Mallard, J. Phys. Chem. Ref. Data 17 (1988) Suppl. 1, 1.
[107] E.P. Wigner, Phys. Rev. 73 (1948) 1002.
[108] G.H. Wannier, Phys. Rev. 90 (1953) 817.
[109] C. Rebick, R.D. Levine, J. Chem. Phys. 55 (1971) 2746.
[110] N. Aristov, P.B. Armentrout, J. Am. Chem. Soc. 108 (1986) 1806.
[111] B.C. Eu, W.S. Liu, J. Chem. Phys. 63 (1975) 592.
[112] R.D. Levine, R.B. Bernstein, Molecular Reaction Dynamics, Oxford, New York, 1974.
[113] W.J. Chesnavich, M.T. Bowers, J. Chem. Phys. 68 (1978) 901.
[114] M. Menzinger, A. Yokozeki, Chem. Phys. 22 (1977) 273.
[115] K. Morokuma, B.C. Eu, M. Karplus, J. Chem. Phys. 51 (1969) 5193.
[116] R.D. Levine, R.B. Bernstein, Chem. Phys. Lett. 11 (1971) 552.
[117] E.K. Parks, A. Wagner, S. Wexler, J. Chem. Phys. 58 (1973) 5502.
[118] A.G. Ureña, Mol. Phys. 5 (1984) 1145.
[119] K.M. Ervin, Int. J. Mass Spectrom. 185/186/187 (1999) 343.
[120] W.J. Chesnavich, M.T. Bowers, J. Phys. Chem. 83 (1979) 900.
[121] R.A. Marcus, J. Chem. Phys. 45 (1966) 2630.
[122] R.G. Gilbert, S.C. Smith, Theory of Unimolecular and Recombination Reactions, Blackwell Scientific, Oxford, 1990.
[123] D.G. Truhlar, B.C. Garrett, S.J. Klippenstein, J. Phys. Chem. 100 (1996) 12771.
[124] K.A. Holbrook, M.J. Pilling, S.H. Robertson, Unimolecular Reactions, 2nd ed., Wiley, New York, 1996.
[125] P.B. Armentrout, in Advances in Gas Phase Ion Chemistry, N.G. Adams, L.M. Babcock (Eds.) JAI, Greenwich, CT, 1992, Vol. 1, p. 83.
[126] G.F. Stowe, R.H. Schultz, C.A. Wight, P.B. Armentrout, Int. J. Mass Spectrom. Ion Processes 100 (1990) 177.
[127] C. Rue, P.B. Armentrout, I. Kretzschmar, D. Schröder, J.N. Harvey, H. Schwarz, J. Chem. Phys. 110 (1999) 7858.
[128] R.A. Dressler, S.T. Arnold, E. Murad, J. Chem. Phys. 103 (1995) 9989.
[129] T. Baer, W.L. Hase, Unimolecular Reaction Dynamics, Oxford, New York, 1996, p. 316, and references therein.
[130] E.J. Heller, R.C. Brown, J. Chem. Phys. 79 (1983) 3336.
[131] J.C. Lorquet, B. Leyh-Nihant, J. Phys. Chem. 92 (1988) 4778.
[132] V.L. Talrose, P.S. Vinogradov, I.K. Larin, in Gas Phase Ion Chemistry, M. T. Bowers (Ed.), Academic, New York, 1979, Vol. 1, p.305.
[133] P.B. Armentrout, J.L. Beauchamp Chem. Phys. 48 (1980) 315.
[134] B.H. Mahan, W.E.W. Ruska, J.S. Winn, J. Chem. Phys. 65 (1976) 3888.
[135] M.E. Weber, J.L. Elkind, P.B. Armentrout, J. Chem. Phys. 84 (1986) 1521.
[136] S.A. Safron, N.D. Weinstein, D.R. Herschbach, J.C. Tully, Chem. Phys. Lett. 12 (1972) 564.
[137] R.C.C. Lao, R.W. Rozett, W.S. Koski, J. Chem. Phys. 49 (1968) 4202.

[138] T.O. Tiernan, R.E. Marcotte, J. Chem. Phys. 53 (1970) 2107.
[139] R J. Cotter, W.S. Koski, J. Chem. Phys. 59 (1973) 784.
[140] P.A.M. van Koppen, A.J. Illies, S. Liu, M.T. Bowers, Org. Mass Spectrom. 17 (1982) 399.
[141] K. Ervin, S.K. Loh, N. Aristov, P.B. Armentrout, J. Phys. Chem. 87 (1983) 3593.
[142] J.L. Elkind, P.B. Armentrout, J. Phys. Chem. 89 (1985) 5626.
[143] J.L. Elkind, P.B. Armentrout, J. Chem. Phys. 84 (1986) 4862.
[144] J.L. Elkind, P.B. Armentrout, J. Phys. Chem. 90 (1986) 5736.
[145] J.L. Elkind, P.B. Armentrout, J. Phys. Chem. 91 (1987) 2037.
[146] K.M. Ervin, P.B. Armentrout, J. Chem. Phys. 85 (1986) 6380.
[147] K.M. Ervin, P.B. Armentrout, J. Chem. Phys. 90 (1989) 118.
[148] J.C. Weisshaar, Adv. Chem. Phys. 82 (1992) 213.
[149] M. Schweizer, S. Mark, D. Gerlich, Int. J. Mass Spectrom. Ion Processes 135 (1994) 1.
[150] D. Gerlich, J. Chem. Phys. 90 (1989) 3574.
[151] D. Gerlich, J. Chem. Soc. Faraday Trans. 89 (1993) 2199.
[152] L.S. Sunderlin, P.B. Armentrout, J. Chem. Phys. 100 (1994) 5639.
[153] V.F. DeTuri, M.A. Su, K.M. Ervin, J. Phys. Chem. A 103 (1999) 1468.
[154] W.A. Chupka, in Ion–molecule Reactions, J. L. Franklin (Ed.), Plenum, New York, 1972, Vol. 1, p. 33.
[155] T. Turner, O. Dutuit, Y.T. Lee, J. Chem. Phys. 81 (1984) 3475.
[156] F.A. Houle, S.L. Anderson, D. Gerlich, T. Turner, Y.T. Lee, J. Chem. Phys. 77 (1982) 748.
[157] B. Yang, Y.-H. Chiu, S.L. Anderson, J. Chem. Phys. 94 (1991) 6459.
[158] Y.-H. Chiu, H. Fu, J.-T. Huang, S.L. Anderson, J. Chem. Phys. 101 (1994) 5410.
[159] R.H. Schultz, K.C. Crellin, P.B. Armentrout, J. Am. Chem. Soc. 113 (1991) 8590.
[160] R.H. Schultz, P.B. Armentrout, Int. J. Mass Spectrom. Ion Processes 107 (1991) 29.
[161] N.F. Dalleska, K. Honma, P.B. Armentrout, J. Am. Chem. Soc. 115 (1993) 12125.
[162] A.J. Cunningham, A.D. Payzant, P. Kebarle, J. Am. Chem. Soc. 94 (1972) 7627.
[163] Y.K. Lau, S. Ikuta, P. Kebarle, J. Am. Chem. Soc. 104 (1982) 1462.
[164] M. Meot-Ner, C.V. Speller, J. Phys. Chem. 90 (1986) 6616.
[165] I. Szabo, Int. J. Mass Spectrom. Ion Phys. 3 (1969) 103.
[166] I. Szabo, Int. J. Mass Spectrom. Ion Phys. 3 (1969) 169.
[167] K.M. Ervin, P.B. Armentrout, J. Chem. Phys. 86 (1987) 2659.
[168] D.A. Hales, L. Lian, P.B. Armentrout, Int. J. Mass Spectrom. Ion Processes 102 (1990) 269.
[169] Collision Spectroscopy, R.G. Cooks (Ed.), Plenum, New York, 1979.
[170] K. Levsen, H. Schwarz, Mass Spectrom. Rev. 2 (1983) 77.
[171] R.A. Yost, C.B. Enke, J. Am. Chem. Soc. 100 (1978) 2274.
[172] R.A. Yost, C.B. Enke, Org. Mass Spectrom. 16 (1981) 171.
[173] For theoretical overviews and references, see chapters by D.J. Diestler, P.J. Kuntz, in Atom–molecule Collision Theory, R.B. Bernstein (Ed.), Plenum, New York, 1979.
[174] J. Bordas-Nagy, K.R. Jennings, Int. J. Mass Spectrom. Ion Processes 100 (1990) 105.
[175] E.K. Parks, J.G. Kuhry, S. Wexler, J. Chem. Phys. 67 (1977) 3014.
[176] S.H. Sheen, G. Dimoplon, E.K. Parks, S. Wexler, J. Chem. Phys. 68 (1978) 4950.
[177] E.K. Parks, S. Wexler, J. Phys. Chem. 88 (1984) 4492.
[178] N.M. Semo, W.S. Koski, J. Phys. Chem. 88 (1984) 5320.
[179] T.F. Magnera, D.E. David, J. Michl, J. Am. Chem. Soc. 111 (1989) 4100.
[180] T.F. Magnera, D.E. David, D. Stulik, R.G. Orth, H.T. Jonkman, J. Michl, J. Am. Chem. Soc. 111 (1989) 5036.
[181] P.J. Marinelli, R.R. Squires, J. Am. Chem. Soc. 111 (1989) 4101.
[182] C.W. Bauschlicher, S.R. Langhoff, H. Partridge, J. Chem. Phys.94 (1991) 2068.
[183] S.R. Langhoff, Bauschlicher, H. Partridge, M. Sodupe, J. Phys. Chem. 95 (1991) 10677.
[184] D. Walter, P.B. Armentrout, J. Am. Chem. Soc. 120 (1998) 3176.
[185] N. Aristov, P.B. Armentrout, J. Phys. Chem. 90 (1986) 5135.
[186] S.K. Loh, D.A. Hales, L. Lian, P.B. Armentrout, J. Chem. Phys. 90 (1989) 5466.
[187] D.A. Hales, P.B. Armentrout, J. Cluster Sci. 1 (1990) 127.
[188] P.A.M. van Koppen, M.T. Bowers, J.L. Beauchamp, D.V. Dearden, ACS Symp. Ser. 428 (1990) 34.
[189] See, for example: M.T. Rodgers, P.B. Armentrout, J. Phys. Chem. A 101 (1997) 1238.
[190] P. de Sainte Claire, W.L. Hase, J. Phys. Chem. 100 (1996) 8190.
[191] W.A. Chupka, J. Chem Phys. 30 (1959) 191.
[192] S.K. Loh, L. Lian, P.B. Armentrout, J. Am. Chem. Soc. 111 (1989) 3167.
[193] F.A. Khan, D.E. Clemmer, R.H. Schultz, P.B. Armentrout, J. Phys. Chem. 97 (1993) 7978.
[194] M.T. Rodgers, K.M. Ervin, P.B. Armentrout, J. Chem. Phys. 106 (1997) 4499.
[195] M.T. Rodgers, P.B. Armentrout, J. Phys. Chem. A 101 (1997) 2614.
[196] P.B. Armentrout, Int. J. Mass Spectrom. 193 (1999) 227.
[197] M.T. Rodgers, P.B. Armentrout, J. Am. Chem. Soc., 122 (2000) 8548.
[198] M.B. More, D. Ray, P.B. Armentrout, J. Am. Chem. Soc. 121 (1999) 417.
[199] M.T. Rodgers, P.B. Armentrout, J. Phys. Chem. A 103 (1999) 4955.
[200] P B. Armentrout, M.T. Rodgers, J. Phys. Chem. A 104 (2000) 2238.
[201] E.D. Glendening, D. Feller, M.A. Thompson, J. Am. Chem. Soc. 116 (1994) 10657.
[202] M.T. Rodgers, P.B. Armentrout, J. Chem. Phys. 109 (1998) 1787.

[203] V.G. DeTuri, K.M. Ervin, J. Phys. Chem. A 103 (1999) 6911.
[204] Y. Shi, K.M. Ervin, Chem. Phys. Lett. 318 (2000) 149.
[205] C.A. Pommerening, S.M. Bachrach, L.S. Sunderlin, J. Am. Soc. Mass Spectrom. 10 (1999) 856.
[206] C.A. Pommerening, S.M. Bachrach, L.S. Sunderlin, J. Phys. Chem. A 103 (1999) 1214.
[207] V.A. Spasov, T.-H. Lee, J.P. Maberry, K.M. Ervin, J. Chem. Phys. 110 (1999) 5208.
[208] V.A. Spasov, T.-H. Lee, K.M. Ervin, J. Chem. Phys. 112 (2000) 1713.
[209] D.H. Mordaunt, M.N. Ashfold, J. Chem. Phys. 101 (1994) 2630.
[210] M.E. Weber, N.F. Dalleska, B.L. Tjelta, E.R. Fisher, P.B. Armentrout, J. Chem. Phys. 98 (1993) 7855.
[211] C.L. Haynes, Y.-M. Chen, P.B. Armentrout, J. Phys. Chem. 99 (1995) 9110.
[212] C.L. Haynes, Y.-M. Chen, P.B. Armentrout, J. Phys. Chem. 100 (1996) 111.
[213] E.R. Fisher, B.L. Kickel, P.B. Armentrout, J. Chem. Phys. 97 (1992) 4859.
[214] M.R. Sievers, Y.-M. Chen, P.B. Armentrout, J. Chem. Phys. 105 (1996) 6322.
[215] I. Kretzschmar, D. Schröder, H. Schwarz, C. Rue, P.B. Armentrout, J. Phys. Chem. A 102 (1998) 10060.